

Sequence Graph Transform (SGT): A Feature Extraction Function for Sequence Data Mining

Chitta Ranjan, Samaneh Ebrahimi, and Kamran Paynabar

H. Milton Stewart School of Industrial and Systems Engineering, Georgia Institute of Technology, Atlanta, GA

Email: {nk.chitta.ranjan,samaneh.ebrahimi,kamran.paynabar}@gatech.edu

Abstract

The ubiquitous presence of sequence data across fields like web, healthcare, bioinformatics, and text mining, has made sequence mining a vital research area. However, sequence mining is particularly challenging because of absence of an accurate and fast approach to find (dis)similarity between sequences. As a measure of (dis)similarity, mainstream data mining methods like k-means, kNN and regression have proved *distance* between data points in a Euclidean space to be most effective. But a distance measure between sequences is not obvious due to their unstructuredness — arbitrary strings of arbitrary length. We, therefore, propose a new function, called Sequence Graph Transform (SGT), that extracts sequence features and embeds them in a finite-dimensional Euclidean space. SGT is *scalable* due to a low computational complexity and has a *universal applicability* to most sequence problem. We theoretically show that SGT can capture both short and long patterns in sequences and provides an accurate distance-based measure of (dis)similarity between them. This is also validated experimentally. Finally, we show its real world application for clustering, classification, search and visualization on different sequence problems.

1 Introduction

A sequence can be defined as a contiguous chain of discrete *alphabets*, where an alphabet can be an event, a value or a symbol, sequentially tied together in a certain order, e.g., BAABCCADECDBBA. Sequences are one of the most common data types found in diverse fields like social science, web, healthcare, bioinformatics, marketing and text mining. Some examples of sequences are: web logs, music listening history, patient movements through hospital wards, DNA, RNA and protein sequences in bioinformatics.

This ubiquitous presence of sequence data has made development of new sequence analysis methods important. Some examples of its applications include: a) understanding users' behavior from their web-surfing and buying sequences data to serve them better advertisements, product placements, promotions, and so on, b) assessing process flows (sequences) in a hospital to find the expected patient movement based on her diagnostic profile, to better optimize the hospital resource and service, and c) analysis of biological sequences to understand human evolution, physiology and diseases.

However, the existing sequence data mining methods lack in their effectiveness due to absence of a good measure of (dis)similarity between sequences. For a (dis)similarity measure, almost all mainstream data mining methods use a *distance* between objects in a Euclidean space. For example, in *k*-means clustering the *distance* between objects (data points) within a cluster are minimized while *distance* between clusters are maximized; in classification models like SVM or logistic regression, the *distance* of a boundary is minimized or maximized from the objects. In deep learning realm as well, objects are transformed into Euclidean vectors for comparisons. It has been commonly accepted that in a Euclidean space, *distance* between objects is one of the best measures of (dis)similarity.

However, since sequences are an unstructured data — made of arbitrarily placed alphabets for any arbitrary length — their representation in a Euclidean space is not obvious. Lack of a Euclidean space representation devoids sequence data analysis from the mainstream data mining methods. This causes sequence mining methods to be less effective, in terms of accuracy, complexity and interpretability.

To that end, feature extraction of sequences in a finite-dimensional Euclidean feature space is necessary. This can also be viewed as an embedding space, where the objective is to transform a sequence into a feature vector, such that the features capture the sequence characteristics. Besides, by definition, the embedding space has the same dimension for all sequences in a data corpus. This will facilitate computation of (dis)similarity between two sequences by measuring the *distance* between their embeddings.

Several researchers proposed feature sets or functions (see references in Kumar et al., 2012) based on a fundamental premise: *a sequence is characterized by the patterns formed due to the alphabets' positions relative to others*. However, to work with this premise some of them make strong assumptions, which are not always valid. For example, Markovian models (Ranjan et al., 2015) typically make a first-order Markov assumption about the sequence generation process. On the other hand, some methods perform information abstraction by taking n-grams or substrings that can potentially lead to a loss of information or inclusion of noise. The existing methods and their shortcomings are elaborated further in the subsequent subsection (Sec. 1.1).

We, therefore, develop a new feature extraction approach, Sequence Graph Transform (SGT), that works on the same fundamental premise but without any restrictive assumptions. Importantly, it effectively captures the sequence features and embeds them into a finite-dimensional Euclidean space that leads to an accurate comparison of sequences by measuring the *distance* between them in the feature space.

In the following, we discuss the related work (Sec. 1.1) and then give the problem specifications, viz. the sequence mining challenges, types of problems and the scope of proposed approach, in Sec. 1.2.

1.1 Related Work

There are several research work in the sequence mining area; a detailed survey can be found in Kumar et al. (2012), Gaber (2009), Dong and Pei (2007), and references therein. In this section, we will briefly go through the broad categories of the literature and discuss their characteristics and shortcomings.

Early research works used *edit*-distances between sequences after alignment. Methods for global alignment, local alignment, with or without overlapping, were developed by Needleman and Wunsch, 1970, Smith and Waterman, 1981. Subsequently, a few heuristic approaches were proposed based on alignment techniques that can work on a larger dataset (BLAST, Altschul et al., 1997, and FASTA, Pearson, 1990). More recently, multiple sequence alignment techniques were developed (UCLUST, Edgar, 2010; CD-HIT, Fu et al., 2012; and MUSCLE, Edgar, 2004). These methods mainly focus on bioinformatics sequence problems and severely lack in their general applicability (*generality*) due to difficulty in tuning, high computational complexity, and inability to work on sequences with significantly varying lengths. Besides, these methods do not provide any feature representation of sequences.

Few researchers worked on sequence features extraction for an embedding in the Euclidean space (Linial et al., 1997, Ding and Dubchak, 2001). But their methods are *ad-hoc* feature spaces developed for protein sequences with no theoretical support; thus they are difficult to extend to a general setting.

More universally applicable and relatively powerful methods work on one of the following broad assumptions, a) the sequence process has an underlying parametric distribution, b) similar sequences have common substrings, and c) a sequence evolves from hidden strings.

The parametric methods typically make Markovian distribution assumptions, more specifically a first-order Markov property, on the sequence process (Cadez et al., 2003 and Ranjan et al., 2015). However, such distributional assumption is not always valid. General n -order Markov models were also proposed but not popular in practice due to high computation. Beyond Markov models, Hidden Markov model-based approaches are popular in both bioinformatics and general sequence problems (HHblits: Remmert et al., 2012; Hlske and Hlske, 2016). It assumes a hidden layer of latent states which results in the observed sequence. These hidden states have a first-order Markov transition assumption, but due to the multi-layer setting, the first-order assumption is not transmitted to the observed sequence. However, tuning HMM (finding optimal hidden states) is difficult and is computationally intensive, thus effecting its *generality* and *scalability*.

N -gram methods (also known as k -mer methods in bioinformatics area) are the most popular approaches that work on the second assumption (Tomović et al., 2006; Hauser et al., 2013). Although the pretext of

this assumption seems appropriate, the optimal selection of substring length, i.e. n in n -gram or k in k -mer, is difficult. In sequence mining, selection of a small value for n can lead to inclusion of noise, but increasing it severely increases the computation. Some other variants, such as spaced-words and adaptive n , are more difficult to optimize (Didier et al., 2012; Comin and Verzotto, 2012).

Another class of methods hypothesize that sequences are generated from some evolutionary process in which a sequence is produced by reproducing complex strings from simpler substrings (Siyari et al., 2016, and references therein). This method solves an NP-hard optimization problem to identify the underlying evolution hierarchy and the corresponding substrings. These substrings can also be used as features for sequence data mining. However, the estimation algorithms for this and similar methods are heuristics that usually do not guarantee optimality. The algorithms can also lead to several solutions which will cause identifiability and ambiguity issues. Moreover, the evolutionary assumption may not be always true.

The above methods either limit the extent of sequence pattern extraction due to restrictive assumptions, or search for (hidden) states or strings in an unobservable universe. This causes a limited accuracy and/or computational issues.

Besides these methods, Prefixspan (Han et. al., 2001) is another sequence pattern mining approach, but it works on different type of sequences where a sequence is a list of elements and each element consists of a set of items, eg. $\langle a(abc)(ac)d(cf) \rangle$. For sequence problems addressed here, Prefixspan’s performance will be similar to n -grams.

Moreover, sequence mining problems have also been given attention by the deep learning research community. Embedding spaces for sequences have been proposed using Recurrent Neural Networks (RNN) and Long Short Term Memory (Graves, 2013). However, the dimension of these embeddings is typically large, and finding the optimal dimension and embeddings require the use of rigorous optimization problems in a deep learning network. Training such models is computationally intensive, sometimes not interpretable and requires a large amount of training data.

1.2 Problem Specification

As discussed above, the related methods fail to address at least one of the following challenges: a) feature mapping: effective extraction of sequence characteristics into a finite-dimensional Euclidean space (a vector), b) universal applicability: this mainly requires absence of any distributional or a domain specific assumption and a small number of tuning hyper-parameters, and c) scalability: it relies on the computational complexity, which should be small with respect to sequence length, size of the database and alphabets set.

We propose a new sequence feature extraction function, called Sequence Graph Transform (SGT), that addresses all of the above challenges and is shown to outperform existing state-of-the-art methods in sequence data mining. SGT works by quantifying the pattern in a sequence by scanning the positions of all alphabets relative to each other. We call it a *graph* transform because of its inherent property of interpretation as a graph, where the alphabets form the nodes and a directed connection between two nodes shows their “association.” These “associations” between all alphabets represent the characteristic features of a sequence. A Markov model transition matrix can be compared analogously with the SGT’s feature space; however, among other differences (explored further in the paper), the associations (graph edges) do not represent a probability, and SGT is non-parametric. The non-parametric property also makes it robust to any underlying sequence generation distribution.

In addition, sequence analysis problems can be broadly divided into: a) *length-sensitive*: the inherent patterns as well as the sequence lengths should match to render two sequences as similar, e.g., in protein sequence clustering, and b) *length-insensitive*: the inherent patterns should be similar, irrespective of the lengths, e.g., weblog comparisons. In contrast with the existing literature, SGT provides a solution for both scenarios. The advantage of this property becomes more pronounced when we have to perform both types of analysis on the same data, and implementing different methods for each becomes cumbersome.

In this paper, our major contribution is the development of a new feature extraction function, SGT, for sequences. We support SGT’s efficacy theoretically, as well as perform an extensive experimental evaluation. Furthermore, we show that SGT bridges the gap between sequence mining and mainstream data mining through implementation of fundamental methods, viz. PCA, k-means, SVM and graph visualization via SGT on real sequence data analysis.

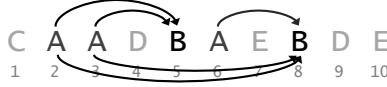


Figure 1: Illustration of effect of elements on each other. In this example, we show effect of presence of A on B.

In the following, we first present the overview and intuition behind SGT, alongwith its formal definition and development(in Sec. 2). We also discuss its characteristics, theoretical properties, extensions, and implementation algorithms in this section. Thereafter, we experimentally validate the efficacy of SGT via clustering and compare it with other state-of-the-art methods. We also show its capability of performing alphabet clustering as an extension. After the validation, we illustrate some real-world applications, viz. clustering, visualization, classification and search, using four different datasets in Sec. 5. Finally, we discuss the results and performance aspects of SGT and conclude in Sec. 6.

2 Sequence Graph Transform (SGT)

2.1 Overview and Intuition

Sequence Graph Transform works on the same fundamental premise — the relative positions of alphabets in a sequence characterize the sequence — to extract the pattern features of the sequence. This premise holds true for most sequence mining problems because similarity in sequences is often measured based on the similarities in their pattern. For commonly occurring feed-forward sequences, this premise is equivalent to: the position of an alphabet instance in a sequence is a result of interactions from all the preceding alphabets instances. For a simpler terminology, we call an alphabet instance an “event.” A feed-forward sequence example can be a clickstream sequence for a user, where any subsequent click event depends on the prior links she clicked. In the following, we will illustrate and develop the feature extraction approach for feed-forward sequences and later show its extension to “undirected” (no forward or reverse directional relationship between consecutive events) sequences.

In an illustrative example in Fig. 1, showing a feed-forward sequence, the presence of alphabet B at positions 5 and 8 should be seen in context with or as a result of all other predecessors. To extract the sequence features, we take relative positions of an alphabet pair at a time. For example, the relative positions for pair (A,B) are $\{(2,3),5\}$ and $\{(2,3,6),8\}$, where the values in the position set for A are the ones preceding B. In the SGT procedure defined and developed in the following sections (Sec. 2.3-2.4), we assay such positions information to extract the sequence features.

These extracted features are “association” between A and B, which can be interpreted as a connection feature representing “A leading to B.” We should note that “A leading to B” will be different from “B leading to A.” This is similar to the Markov probabilistic models, in which transition probabilities of going from A to B is estimated. However, it is different because the connection feature 1) is not a probability, and 2) takes into account all orders of relationship without any increase in computation.

The extracted association between A and B can also be interpreted as a measure of separation (or closeness) between A to B. Again, the separation going from A to B will be different from B to A. The associations between all alphabets in alphabet set, denoted as \mathcal{V} , can be extracted similarly to obtain sequence features in a $|\mathcal{V}|^2$ -dimensional feature space. Besides, in contrast to the evolutionary or hidden layer models, SGT will not require search for any hidden states or strings.

The SGT features also make it easy to visualize the sequence as a directed graph, with sequence alphabets in \mathcal{V} as graph nodes and the edge’s weights equal to the directional association between nodes. Hence, we call it a sequence *graph* transform. Moreover, we show that under certain conditions the SGT also allows node clustering, which is the alphabet clustering.

A high level overview of our approach is given in Fig. 2a-2b. In Fig. 2a we show that applying SGT on a sequence, s , yields a finite-dimensional feature vector, $\Psi^{(s)}$, for the sequence, also interpreted and visualized as a directed graph. For a general sequence data analysis, SGT can be applied on each sequence in a data corpus, as shown in Fig. 2b, to yield a finite- and equal-dimensional representation corresponding to each

sequence. This provides a direct distance-based comparison between sequences and thus makes application of mainstream data mining methods for sequence analysis rather straightforward.

2.2 Notations

Suppose we have a dataset of sequences denoted by \mathcal{S} . Any sequence in the dataset, denoted by $s(\in \mathcal{S})$, is made of alphabets in set \mathcal{V} . A sequence can have instances of one or many alphabets from \mathcal{V} . For example, sequences from a dataset, \mathcal{S} , made of alphabets in, $\mathcal{V} = \{A, B, C, D, E\}$ (suppose), can be $\mathcal{S} = \{AABAAABCC, DEEDE, ABBDECCABB, \dots\}$. As we can see, the sequences in the set have instances of $\{A, B, C\}$, $\{D, E\}$, $\{A, B, C, D, E\} \subseteq \mathcal{V}$, respectively. The length of a sequence, s , denoted by $L^{(s)}$, is equal to the number of events in it. In the sequence, s_l will denote the alphabet at position l , where $l = 1, \dots, L^{(s)}$ and $s_l \in \mathcal{V}$.

As mentioned in the previous section, we extract sequence features in the form of “associations” between the alphabets, represented as $\psi_{uv}^{(s)}$, where $u, v \in \mathcal{V}$, are the corresponding alphabets, and ψ is a function of ϕ . ϕ is also a function that takes a “distance,” d , as an input and κ as a tuning hyper-parameter, represented as $\phi_{\kappa}(d)$.

Note that $\psi_{uv}^{(s)} \neq \psi_{vu}^{(s)}$ for feed-forward sequences. The connection features, $\Psi^{(s)} = [\psi_{uv}^{(s)}], u, v \in \mathcal{V}$, can be interpreted as a directed “graph”, with edge weights, ψ , and nodes in \mathcal{V} , or is vectorized to a $|\mathcal{V}|^2$ -vector denoting the sequence s in the feature space. Each sequence, $s \in \mathcal{S}$, is transformed to this feature space to get $\Psi^{(s)}, \forall s \in \mathcal{S}$.

2.3 SGT Definition

As also explained in Sec. 2.1, the Sequence Graph Transform extracts the features from the relative positions of events (alphabet instances). A quantification for an “effect” from relative positions of two events in a sequence is given by $\phi(d(l, m))$, where l, m are the positions of the events and $d(l, m)$ is a distance (or gap) measure. This quantification is a directional effect of the preceding event on the later event. For example, see Fig. 3a, where u and v are at positions l and m , and the directed arc denotes the effect of u on v .

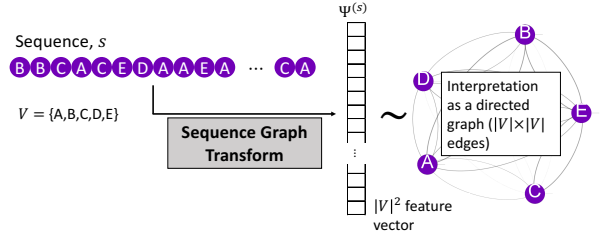
For developing SGT, we require following conditions on ϕ , a) Strictly greater than 0: $\phi_{\kappa}(d) > 0; \forall \kappa > 0, d > 0$; b) Strictly decreasing with d : $\frac{\partial}{\partial d} \phi_{\kappa}(d) < 0$; and c) Strictly decreasing with κ : $\frac{\partial}{\partial \kappa} \phi_{\kappa}(d) < 0$.

The first condition is to keep the extracted feature, $\psi = f(\phi)$, easy to analyze and interpret. The second condition strengthens the effect of closer neighbors. The last condition helps in tuning the procedure, allowing us to change the effect of neighbors.

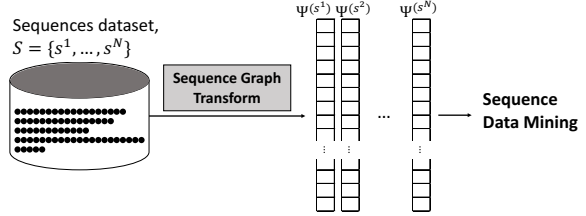
There are several functions that satisfy the above conditions, e.g., Gaussian, Inverse, and Exponential. Also, $d(l, m)$ is a distance function, taken as $|m - l|$ in this paper. Besides, ϕ is taken as an exponential function because it will yield interpretable results for the SGT properties (Sec. 2.4). Thus,

$$\phi_{\kappa}(d(l, m)) = e^{-\kappa d(l, m)} = e^{-\kappa |m - l|}, \forall \kappa > 0, d > 0 \quad (1)$$

In a general sequence, we will have several instances of an alphabet pair. For example, see Fig. 3b, where there are five (u, v) pairs, and an arc for each pair shows an effect of u on v . Therefore, the first step is to



(a) Feature extracted as a vector with a graph interpretation.



(b) Use of sequences' SGT features for data mining

Figure 2: Overview of SGT feature extraction and data mining procedure.

Each sequence, $s \in \mathcal{S}$, is transformed to this feature



Figure 3: Visual illustration of effect of alphabets' relative positions.

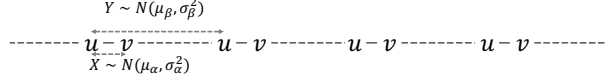


Figure 4: Representation of short- and long-term pattern

find the number of instances of each alphabet pair. The instances of alphabet pairs are stored in a $|\mathcal{V}| \times |\mathcal{V}|$ asymmetric matrix, Λ . Here, Λ_{uv} will have all instances of alphabet pairs (u, v) , such that in each pair instance, v 's position is after u .

Thus,

$$\Lambda_{uv}(s) = \{(l, m) : s_l = u, s_m = v, l < m, (l, m) \in 1, \dots, L^{(s)}\} \quad (2)$$

In the sequence, ϕ from each (u, v) pair instance will contribute to the ‘‘association’’ feature, ψ_{uv} . Thus, we aggregate individual contributions from each pair instance and normalize it, as shown below in Eq. 3a-3b, to give ψ_{uv} . Here, $|\Lambda_{uv}|$ is the size of the set Λ_{uv} , which is equal to the number of (u, v) pair instances. Eq. 3a gives the feature expression for a *length-sensitive* sequence analysis problem because it also contains the sequence length information within it (proved with a closed-form expression under certain conditions in the following, Sec. 2.4). In Eq. 3b, the length effect is removed by standardizing $|\Lambda_{uv}|$ with the sequence length $L^{(s)}$ for *length-insensitive* problems.

$$\psi_{uv}(s) = \frac{\sum_{\forall(l,m) \in \Lambda_{uv}(s)} e^{-\kappa|m-l|}}{|\Lambda_{uv}(s)|}; \text{ length sensitive} \quad (3a)$$

$$\psi_{uv}(s) = \frac{\sum_{\forall(l,m) \in \Lambda_{uv}(s)} e^{-\kappa|m-l|}}{|\Lambda_{uv}(s)|/L^{(s)}}; \text{ length insensitive} \quad (3b)$$

and $\Psi(s) = [\psi_{uv}(s)]$, $u, v \in \mathcal{V}$ is the SGT feature representation of sequence s .

For illustration, the SGT feature for alphabets pair (A,B) in sequence in Fig. 1 can be computed as (for $\kappa = 1$ in length-sensitive SGT): $\Lambda_{AB} = \{(2, 5); (3, 5); (2, 8); (3, 8); (6, 8)\}$ and $\psi_{AB} = \frac{\sum_{\forall(l,m) \in \Lambda_{AB}} e^{-|m-l|}}{|\Lambda_{AB}|} = \frac{e^{-|5-2|} + e^{-|5-3|} + e^{-|8-2|} + e^{-|8-3|} + e^{-|8-6|}}{5} = 0.066$.

The developed SGT effectively extracts the pattern features of a sequence leading to an accurate comparison of different sequences. In the next section, we will prove this efficacy.

2.4 SGT properties

In this section, we show SGT's property of capturing both short- and long-term sequence pattern features. This is shown by a closed-form expression for the SGT feature, ψ_{uv} , under some mild assumptions. Note that the assumptions made in this section are only for showing an interpretable expression and are not required in practice.

The assumption and proposition are given as follows.

Assumptions: For a sequence with an inherent pattern: ‘‘ u, v occurs closely together with a stochastic gap between, $X \sim N(\mu_\alpha, \sigma_\alpha^2)$, and the intermittent stochastic gap between the pairs as, $Y \sim N(\mu_\beta, \sigma_\beta^2)$, such that, $\mu_\alpha < \mu_\beta$ ’’ (See Fig. 4).

$X \sim N(\mu_\alpha, \sigma_\alpha^2)$ and $Y \sim N(\mu_\beta, \sigma_\beta^2)$ characterizes the short- and long-term patterns, respectively. Given this, the expected number of immediate (u, v) pairs is proportional to the sequence length, L , with a proportionality constant denoted by p .

Proposition: SGT feature has a closed-form expression which shows that it captures both short- and long-term patterns present in a sequence in both length-sensitive and -insensitive SGT variants (derived in Appendix-B).

Length-sensitive

The expected value of SGT feature, ψ_{uv} , is,

$$E[\psi_{uv}] = \frac{2}{pL+1}\gamma \quad (4)$$

Length-insensitive

$$E[\psi_{uv}] = \frac{2L}{pL+1}\gamma \quad (5)$$

where,

$$\gamma = \left| \frac{e^{-\tilde{\mu}_\alpha}}{(1 - e^{-\tilde{\mu}_\beta}) \left[1 - \frac{1 - e^{-pL\tilde{\mu}_\beta}}{pL(e^{\tilde{\mu}_\beta} - 1)} \right]} \right| \quad (6)$$

and, $\tilde{\mu}_\alpha = \kappa\mu_\alpha - \frac{\kappa^2}{2}\sigma_\alpha^2$; $\tilde{\mu}_\beta = \kappa\mu_\beta - \frac{\kappa^2}{2}\sigma_\beta^2$. Also, $\lim_{L \rightarrow \infty} \text{var}(\psi_{uv}) \rightarrow 0$.

As we can see in Eq. 4 and 5, the expected value of the SGT feature is proportional to the term γ . And, on looking at γ , we can note that its numerator contains the information about the short-term pattern, and its denominator has the long-term pattern information.

Looking closely, we can observe that if either of μ_α (the closeness of u and v in short-term) and/or μ_β (the closeness of u and v in long-term) decreases, γ will increase, and vice versa. This emphasizes two properties: a) the SGT feature is affected by changes in both short- and long-term patterns, and b) the graph interpretation of SGT is further proven: the SGT feature ψ_{uv} that denotes the weight on the edge connecting the nodes u and v (in the SGT graph) increases if closeness between u, v increases in the sequence (i.e. μ_α and μ_β decrease) the edge weight increases in the SGT graph, indicating the nodes becoming closer in the graph space (and vice versa).

Furthermore, the length-sensitive SGT feature expectation in Eq. 4 contains the sequence length, L . This shows that the SGT feature has the information of sequence pattern, as well as the sequence length. This enables an effective length-sensitive sequence analysis because sequence comparisons via SGT will require both patterns and sequence lengths to be similar.

In the length-insensitive SGT feature expectation in Eq. 5, it is straightforward to show that it becomes independent of the sequence length as the length increases. Therefore, as sequence length, L , increases, the (u, v) ‘‘association’’ feature approaches a constant,

$$\lim_{L \rightarrow \infty} E[\psi_{uv}] \rightarrow \frac{2}{p} \left| \frac{e^{-\tilde{\mu}_\alpha}}{1 - e^{-\tilde{\mu}_\beta}} \right| \quad (7)$$

Besides, as shown in Appendix-B, $\lim_{L \rightarrow \infty} \text{var}(\psi_{uv}) \xrightarrow{1/L} 0$. Thus, the expected value of the SGT feature becomes independent of the sequence length at a rate of inverse to the length. In our experiments, it is observed that the SGT features approaches a length-invariant constant when $L > 30$.

$$\lim_{L \rightarrow \infty} \Pr \left\{ \psi_{uv} = \frac{2}{p} \left| \frac{e^{-\tilde{\mu}_\alpha}}{1 - e^{-\tilde{\mu}_\beta}} \right| \right\} \xrightarrow{1/L} 1 \quad (8)$$

Furthermore, if the pattern variances, σ_α^2 and σ_β^2 in the above scenario, are small, κ allows regulating the feature extraction: higher κ reduces the effect from long-term patterns and vice versa.

The properties discussed above play an important role in SGT’s effectiveness. Due to these properties, unlike the methods discussed in Sec. 1.1, SGT can capture higher orders of relationship without any increase in computation. Besides, SGT can effectively find sequence features without the need for any hidden string/state(s) search.

2.5 Extensions of SGT

2.5.1 Undirected sequences

SGT can be further extended to work on undirected sequences. In such sequences, the directional pattern or directional relationships (as in feed-forward) is not important. In other words, it is immaterial whether B occurs before or after A ; occurring closely (or farther) is important. Here we are interested in overall proximity of events in either direction to characterize a sequence’s pattern. From SGT’s operation standpoint, we have to remove the condition, $l < m$, from Eq. 2, giving us,

$$\tilde{\Lambda}_{uv}(s) = \{(l, m) : s_l = u, s_m = v, (l, m) \in 1, \dots, L^{(s)}\} \quad (9)$$

Thus, the SGT for undirected sequences can be computed and denoted as $\tilde{\Psi}$.

It is easy to show that.

$$\tilde{\Lambda} = \Lambda + \Lambda^T \quad (10)$$

and (see Appendix C for proof),

$$\tilde{\Psi} = \frac{|\Lambda|\Psi + |\Lambda^T|\Psi^T}{|\Lambda| + |\Lambda^T|} \quad (11)$$

where, Λ and Ψ are given in Eq. 2 and Eq. 3a-3b, respectively.

Moreover, for sequences with uniform marginal distribution of occurrence of elements, $v \in \mathcal{V}$, Λ will be close to symmetric; thus, the undirected sequence graph can be approximated as,

$$\tilde{\Psi} \approx \frac{\Psi + \Psi^T}{2} \quad (12)$$

In practice, this approximation is useful in most cases.

2.5.2 Alphabet clustering

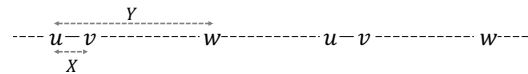
Node clustering in graphs is a classical problem solved by various techniques, such as spectral clustering, graph partitioning and others. SGT’s graph interpretation facilitates grouping of alphabets that occur closely via any of these node clustering methods.

This will effectively require the SGT to give larger weights to the edges, ψ_{uv} , corresponding to alphabet pairs that occur closely. For instance, consider a sequence in Fig. 5a, in which v occurs closer to u than w , also implying $E[X] < E[Y]$. Therefore, in this sequence’s SGT representation, edge weight for $u \rightarrow v$ should be greater than for $u \rightarrow w$, i.e. $\psi_{uv} > \psi_{uw}$. Note that the feature ψ_{uv} is same as the edge weight for arc $u \rightarrow v$ in the graph interpretation.

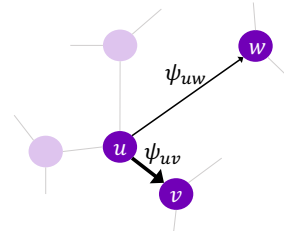
Using the same assumptions as in Sec. 2.4, we will have, $E[|\Lambda_{uv}|] = E[|\Lambda_{uw}|]$. Therefore, $\psi_{uv} \propto E[\phi(X)]$ and $\psi_{uw} \propto E[\phi(Y)]$, and due to Condition 2 on ϕ given in Sec. 2.3,

$$\begin{aligned} \text{if } & E[X] < E[Y] \\ \implies & E[\phi(X)] > E[\phi(Y)] \\ \implies & E[\psi_{uv}] > E[\psi_{uw}] \end{aligned}$$

Moreover, for an easier clustering, it is important to bring the “closer” alphabets more close in the Euclidean space and vice versa. In the SGT’s graph interpretation for the above example, it implies ψ_{uv} should



(a) u, v are closer than u, w .



(b) Corresponding SGT’s Graph view.

Figure 5: Illustrative sequence example for alphabet clustering.

go as high as possible to bring v closer to u in the graph and vice versa for (u, w) . Thus, effectively, $\Delta = E[\psi_{uv} - \psi_{uw}]$ should be increased.

As proved in Appendix D, Δ will increase with the hyper-parameter κ , if we select κ such that $\kappa d > 1$ holds for any value of d . Since d in this case is the relative gap-distance between sequence events, it is always a positive integer. Therefore, the criteria for κ should hold for any $d \in \mathbb{N}$.

Thus, a SGT can represent a sequence as a graph with its alphabets connected with weighted edges, which enables clustering of closely occurring alphabets using graph node clustering methods.

3 SGT Algorithm

In this section, we provide two algorithms for SGT computation. Both algorithms are designed for a feed-forward sequence defined in Eq. 3a-3b and developed with an exponential function for ϕ given in Eq. 1. The two algorithms are for the following two cases to achieve faster computation: 1) Algorithm1 when the sequence lengths are smaller than the feature space, i.e. $L < |\mathcal{V}|^2$, and 2) Algorithm2 when $L > |\mathcal{V}|^2$. However, the second algorithm will require an additional pre-processing of a sequence.

The algorithms take in a sequence, s , from the corpus of sequence database, \mathcal{S} , alphabet set, \mathcal{V} , and the SGT hyper-parameter, κ . We initialize two $\mathcal{V} \times \mathcal{V}$ matrices, $\mathbf{W}^{(0)}$ and $\mathbf{W}^{(\kappa)}$, with zero values, where a $\mathcal{V} \times \mathcal{V}$ matrix is a square matrix of dimension $|\mathcal{V}|$ and the row and column index names are same as the set \mathcal{V} . Besides, the sequence length, L , is initialized as 1 in Algorithm-1, while 0 for Algorithm2. Post computation, $\mathbf{W}^{(0)}$ will correspond to the denominator and $\mathbf{W}^{(\kappa)}$ to the numerator in Eq. 3a-3b.

Algorithm1 parses the input sequence across its length using a nested loop and updates $\mathbf{W}^{(0)}$ and $\mathbf{W}^{(\kappa)}$. Thereafter, if the problem is *length insensitive*, each cell in $\mathbf{W}^{(0)}$ is normalized by dividing by L . Finally, an element-wise division of $\mathbf{W}^{(\kappa)}$ by $\mathbf{W}^{(0)}$ gives the SGT defined in Eq. 3a-3b. However, we output the κ^{th} root of it as the final SGT features because, although the κ^{th} root is not necessary theoretically, it keeps the SGTs easy to interpret and comparable for any value of κ .

In Algorithm2, instead of parsing the sequence length, we perform a nested loop on all alphabets in \mathcal{V} to update $\mathbf{W}^{(0)}$ and $\mathbf{W}^{(\kappa)}$. For that, we pre-process the sequence to obtain a list containing the positions for each alphabet by using the defined function GETALPHABETPOSITIONS. Thereafter, for any pair of alphabets (u, v) we take the set of their positions in the sequence, U and V . We then assign a set C as the cartesian product of sets U and V with a condition that in any resulting pair the position value from set V should be higher than the one from set U . Thus, the cell (u, v) for $\mathbf{W}^{(0)}$ will be equal to the number of tuples in set C , and for $\mathbf{W}^{(\kappa)}$ will be the sum over all results of function ϕ_κ on the difference between elements of each tuple in C . The remaining steps are same as Algorithm1.

For the SGT extension to undirected sequences in Sec. 2.5.1, the loop range in line 3 in Algorithm1 should be changed to $j \in \{1, \dots, \text{length}(s)\}$ and the set assignment in line 13 in Algorithm2 should change to $C \leftarrow U \times V = \{(i, j) | i \in U, j \in V\}$.

The outputted SGT for the sequence, s , will be a $|\mathcal{V}| \times |\mathcal{V}|$ matrix, which can be vectorized (size, $|\mathcal{V}|^2$) for use in distance-based data mining methods, or can be used as is for visualization and interpretation purposes. Moreover, for a sequence dataset, \mathcal{S} , the algorithm should be repeated for all sequences to obtain their feature representations.

Algorithm 1 Parsing a sequence to extract the SGT features

Input: A sequence, $s \in \mathcal{S}$, alphabet set, \mathcal{V} , and hyper-parameter, κ .

```

1: Initialize:
    $\mathbf{W}^{(0)}, \mathbf{W}^{(\kappa)} \leftarrow \mathbf{0}_{\mathcal{V} \times \mathcal{V}}$ , and sequence length,
    $L \leftarrow 1$ 
2: for  $i \in \{1, \dots, (\text{length}(s) - 1)\}$  do
3:   for  $j \in \{(i + 1), \dots, \text{length}(s)\}$  do
4:      $\mathbf{W}_{s_i, s_j}^{(0)} \leftarrow \mathbf{W}_{s_i, s_j}^{(0)} + 1$ 
5:      $\mathbf{W}_{s_i, s_j}^{(\kappa)} \leftarrow \mathbf{W}_{s_i, s_j}^{(\kappa)} + \exp(-\kappa|j - i|)$ 
6:     where,  $s_i, s_j \in \mathcal{V}$ 
7:   end for
8:    $L \leftarrow L + 1$ 
9: end for
10: if length-sensitive is True then
11:    $\mathbf{W}^{(0)} \leftarrow \mathbf{W}^{(0)} / L$ 
12: end if

```

Output $\psi_{uv}(s) \leftarrow \left(\frac{\mathbf{W}_{u,v}^{(\kappa)}}{\mathbf{W}_{u,v}^{(0)}} \right)^{\frac{1}{\kappa}}; \Psi(s) = [\psi_{uv}(s)], (u, v) \in \mathcal{V}$

Algorithm 2 Extract SGT features by scanning alphabet positions of a sequence

Input: A sequence, $s \in \mathcal{S}$, alphabet set, \mathcal{V} , and hyperparameter, κ .

```
1: function GETALPHABETPOSITIONS( $s, \mathcal{V}$ )
2:   positions  $\leftarrow \{\emptyset\}$ 
3:   for  $v \in \mathcal{V}$  do
4:     positions( $v$ )  $\leftarrow \{i : s_i = v, i = 1, \dots, \text{length}(s)\}$ 
5:   end for
6:   return positions
7: end function

8: Initialize:
    $\mathbf{W}^{(0)}, \mathbf{W}^{(\kappa)} \leftarrow \mathbf{0}_{\mathcal{V} \times \mathcal{V}}$ , and sequence length,  $L \leftarrow 0$ 
   positions  $\leftarrow$  GETALPHABETPOSITIONS( $s, \mathcal{V}$ )
9: for  $u \in \mathcal{V}$  do
10:   $U \leftarrow$  positions( $u$ )
11:  for  $v \in \mathcal{V}$  do
12:     $V \leftarrow$  positions( $v$ )
13:     $C \leftarrow (U \times V)^+ = \{(i, j) | i \in U, j \in V, \& j > i\}$ 
14:     $\mathbf{W}_{u,v}^{(0)} \leftarrow \text{length}(C)$ 
15:     $\mathbf{W}_{u,v}^{(\kappa)} \leftarrow \text{sum}(\exp(-\kappa |C_{:,u} - C_{:,v}|))$ 
16:  end for
17:   $L \leftarrow L + \text{length}(U)$ 
18: end for
19: if length-sensitive is True then
20:    $\mathbf{W}^{(0)} \leftarrow \mathbf{W}^{(0)} / L$ 
21: end if
```

Output SGT: $\psi_{uv}(s) \leftarrow \left(\frac{W_{u,v}^{(\kappa)}}{W_{u,v}^{(0)}} \right)^{\frac{1}{\kappa}}$; $\Psi(s) = [\psi_{uv}(s)], (u, v) \in \mathcal{V}$

The time complexity of Algorithm1 is $O(NL^2)$, where N is the number of sequences ($= |\mathcal{S}|$) and L is the average sequence length and $O(N|\mathcal{V}|(L + |\mathcal{V}|))$ for Algorithm2. The space complexity for both is $O(N|\mathcal{V}|^2)$. However, in most datasets, not all alphabets in \mathcal{V} are present in a sequence, resulting into a sparse SGT features representation. In such cases, the complexities reduce by factor of the sparsity level. Moreover, as also evident from Fig. 2b, the SGT operation on any sequence in a dataset is independent of other. This means we can easily parallelize the SGT operation on the sequences in \mathcal{S} to significantly reduce the runtime.

The optimal selection of the hyper-parameter κ will depend on the problem in hand. If the end objective is building a supervised learning model, methods like cross-validation can be used. For unsupervised learning, any goodness-of-fit criteria can be used for the selection. In cases of multiple parameter optimization, e.g. the number of clusters (say, n_c) and κ together in an unsupervised learning, we can use a random search procedure. In such a procedure, we randomly initialize n_c , compute the best κ based on some goodness-of-fit measure, then fix κ to find the best n_c , and repeat until there is no change. From our experiments on real and synthesized data, the results of SGT-based data mining are not sensitive to minor differences in κ . In our implementations, we typically selected κ from $\{1, 5, 10\}$.

4 Experimental Analysis

In this section, we perform an experimental analysis to assess the performance of the proposed SGT. The most important motivation behind SGT is the need for an accurate method to find (dis)similarity between sequences. Therefore, to test SGT’s efficacy in finding sequence (dis)similarities, we built sequence clustering experimental setup. A clustering operation requires accurate computation of (dis)similarity between objects and thus is a good choice for efficacy assessment.

We perform four types of experiments: a) Exp-1: length-sensitive, b) Exp-2: length-insensitive with non-

parametric sequence pattern, c) Exp-3: length-insensitive with parametric sequence pattern, and d) Exp-4: alphabet clustering. The settings for each of them are given in Table 1. Alphabet set is, $\mathcal{V} = \{A, B \dots, Z\}$, for all sequences. Besides, except for Exp-3, clustered sequences were generated, such that sequences within a cluster share common patterns. Here two sequences having a common pattern primarily means the sequences have some common subsequences of any length, and these subsequences can be present anywhere in the sequence. The sequences also comprise of other events, which can be either *noise* or some other pattern. This setting is non-parametric; however, the subsequences can also bring some inherent parametric properties, like a mixture of Markov distribution of different orders. In Exp-3, clustered sequences were generated from a mixture of parametric distributions, such as Markov and Hidden Markov models. In all the experiments, k-means with manhattan distance was applied on SGT representations of the sequences.

In Exp-1, we compare SGT with length-sensitive algorithms, viz. MUSCLE, UCLUST and CD-HIT, which are popular in bioinformatics. These methods are hierarchical in nature, and thus, themselves find the optimal number of clusters. For SGT-clustering, the number of clusters is found using the random search procedure recommended in Sec. 3. Besides, other methods, such as Optimal Matching (e.g. Needleman-Wunsch) or sequence alignment (e.g. Smith-Waterman), are not considered due to their high time complexity, which makes them inappropriate for most large sequence datasets.

Fig. 6 shows the results, where the y axis is the ratio of the estimated optimal number of clusters, \hat{n}_c , and the true number of clusters, n_c . On the x axis, it shows the clustering accuracy, i.e. the proportion of sequences assigned to a same cluster given that they were actually from the same cluster. For a best performing algorithm, both metrics should be close to 1. As shown in the figure, CD-HIT overestimated the number of clusters by about twice, while UCLUST severely overestimated by 5 times, but both had a 100% accuracy. MUSCLE accurately estimated n_c but had about 95% accuracy. On the other hand, SGT could accurately estimate n_c and it also has a 100% clustering accuracy.

In Exp-2, we compare SGT with commonly used sequence or string analysis techniques, viz. n-gram, mixture Hidden Markov model (HMM), Markov model (MM) and semi-Markov model (SMM) based clustering. For n-gram, we take $n = \{1, 2, 3\}$, and their combinations. Note that 1-gram is equivalent to bag-of-words method. For these methods, we provided the known n_c to the algorithms. We use F1-score as the accuracy metric. It considers both the *precision*¹ and the *recall*² of the test to compute the score by taking a weighted average of both, where its best value is 1 and its worst at 0.

Besides, in this experiment, we set different scenarios such that the overlap of clusters’ “centroid” is increased. A high overlap between clusters implies the sequences belonging to these clusters have a higher number of common patterns. Thus, separating them for clustering becomes difficult, and clustering accuracy is expected to be lower.

Fig. 7a shows the accuracy results for the above experimentation. As shown in the figure, SGT-clustering always has a higher accuracy (F1-score) and is significantly higher than MM and SMM. This is due to the fact that both MM and SMM work on a first-order Markov distribution assumption on sequences. On the other hand, although HMM has a first-order Markov assumption on the hidden states, the observed sequence events do not require such condition. Therefore, in comparison to the MM and SMM, HMM’s accuracy is relatively more robust to the strict distribution assumptions on a sequence. As a result, we see its F1-score to be comparable to SGT. The n-gram methods lie in between. An interesting finding is, while higher order

	Sequence length, μ, σ	Noise level	#clusters, n_c
Exp-1	424.6, 130.6	45-50%	5
Exp-2	116.4, 47.7	35-65%	5
Exp-3	98.2, 108.3	–	5
Exp-4	103.9, 33.6	30-50%	3

Table 1: Experimentation settings

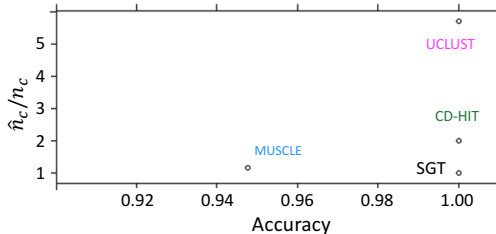


Figure 6: Exp-1 on length-sensitive sequence problem.

¹Precision is the number of correct positive results divided by the number of all positive results.

²Recall is the number of correct positive results divided by the number of positive results that should have been returned.

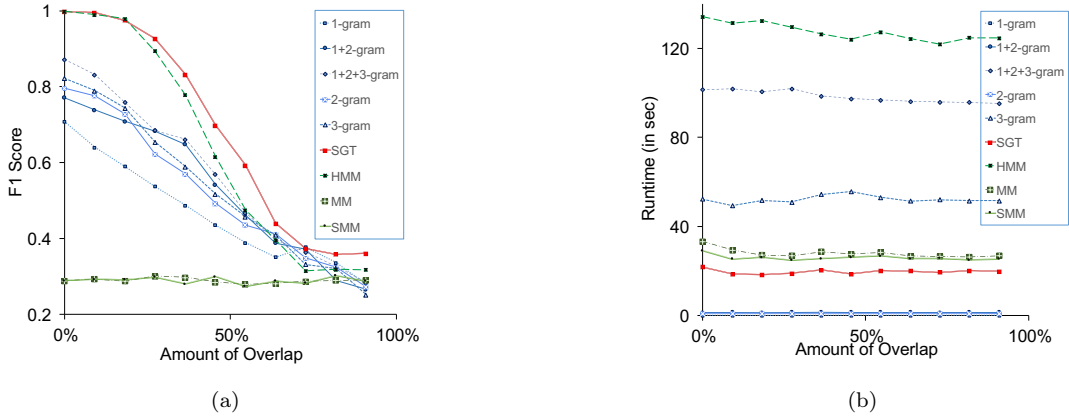


Figure 7: Experimentation results for general sequence datasets to compare the efficiency of sequence clustering methods. Higher overlap implies the sequences, belonging to different clusters, share many patterns and, therefore, are harder to separate.

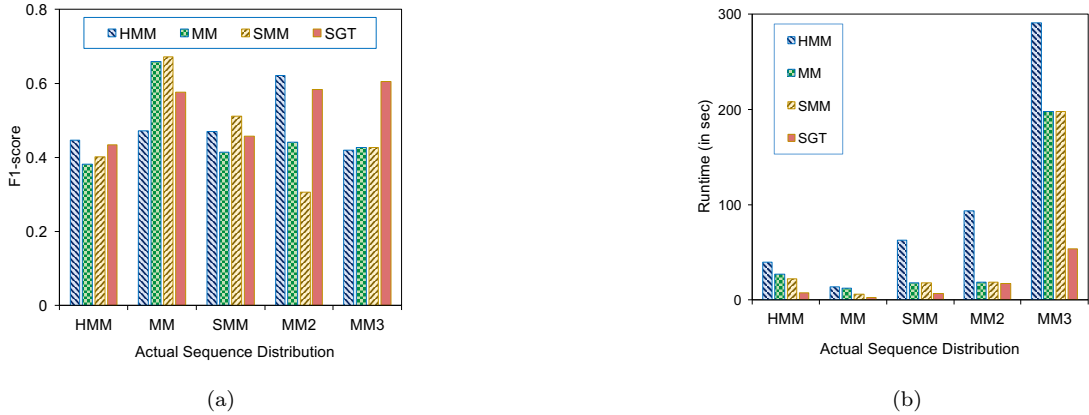


Figure 8: Efficacy validation of proposed SGT method on experimental datasets synthesized from different parametric distributions. For each parametric dataset, all parametric and proposed SGT methods are compared.

n-grams performed better in general, the 1-gram method is better when overlapping was high. This shows higher order n-grams inability to distinguish between sequences when patterns are very similar.

Besides, in Fig. 7b the runtimes of the methods are compared. The smaller order n-grams have very low runtime. Among others, HMM has significantly higher runtime while SGT has lowest.

Furthermore, we did Exp-3 to see the performance of SGT in sequence datasets having an underlying mixture of parametric distributions, viz. mixture of HMM, MM and SMM. The objective of this experimentation is to test SGT’s efficacy on parametric datasets against parametric methods. In addition to obtaining datasets from mixed HMM and first-order mixed MM and SMM distributions we also get second-order Markov (MM2) and third-order Markov (MM3) datasets. As expected, the mixture clustering method corresponding to the underlying distribution is performing the best. Note that SMM is slightly better than MM in the MM setting because of its over-representative formulation, i.e. a higher dimensional model to include a variable time distribution. However, the proposed SGT’s accuracy is always close to the best. This shows SGT’s robustness to underlying distribution and its universal applicability. Besides, again, its runtime is smaller than all others.

Finally, we validate the efficacy of the extensions of SGT given in Sec. 2.5 in Exp-4. Our main aim in this validation is to perform alphabet clustering (Sec. 2.5.2). We setup a test experiment such that across different sequence clusters some alphabets occur closer to each other. We create a dataset that has sequences from three clusters and alphabets belonging to two clusters (alphabets, A-H in one cluster and I-P in another). There are

common patterns between sequences in a cluster and the patterns are such that alphabets from same alphabet cluster will be closer. For eg. a cluster can have patterns like {EFEACDAA, FGGCA, NNKLI, KJJOO LLPM, ...}, where a pattern maintains the closeness of alphabets imposed from their underlying true group.

This emulates a biclustering scenario where sequences in different clusters will have distinct patterns, however, the pattern of closely occurring alphabets is common across all sequences. This is a complex scenario where clustering both sequences and alphabets can be challenging. In a typical real world problem, the alphabet clusters can be expected to be distinct in different sequence clusters, where the bi-clustering can be done in two stages, 1) cluster sequences, 2) for each sequence cluster, cluster the alphabets. Nevertheless, in this experiment we show that the developed SGT can be used to perform the bi-clustering together on a complex dataset.

In this experiment, we assume that it is required to group the alphabets by, a) finding closeness between *distinct* alphabets, and b) irrespective of their directional pattern. For the former, we include SGT extension in Sec. 2.5.2 and the extension in Sec. 2.5.1 for the latter. This setup will validate the SGT extensions together. However, the accuracy will remain unaffected even if the analysis is done without the above two assumptions and, in turn, extensions.

Upon clustering the sequences, the F1-score is found as 1.0. . For alphabets clustering, we applied spectral clustering on the aggregated SGT's of all sequences, which yielded an accurate result with only one alphabet as mis-clustered. Moreover, a heatmap in Fig. 9 clearly shows that alphabets within same underlying clusters have significantly higher associations. Thus, it validates that SGT can accurately cluster alphabets together with clustering the sequences.

In this section, we showed that SGT outperforms existing methods in terms of both accuracy and runtime. This validates the premise that SGT is an effective representation of sequences, that precisely characterizes a sequence's patterns, and thus, provides accurate distance-based (dis)similarities for sequence data mining.

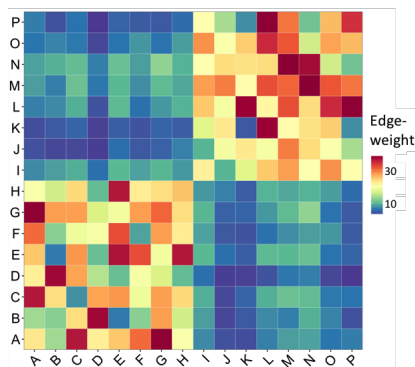


Figure 9: Heat-map showing alphabets' association via SGT edge-weights.

5 Applications

In this section we show few applications of SGT based sequence mining on real world datasets. We use four datasets, two from protein databases, one computer network log data and a user web navigation data. We show that SGT facilitates use of mainstream data mining for sequences and, indeed, outperforms the commonly used sequence mining methods.

5.1 Clustering

Sequence clustering is an important application area across various fields. One important problem in this area is clustering user activity on web (web log sequences) to understand their behavior. This analysis helps in better service, design, advertisements and promotions.

We take a user navigation data³ on msnbc.com collected during a 24-hour period. The navigation data are weblogs that correspond to page views of each user. The alphabets of these sequences are the events corresponding to a user's page request. These requests are recorded at a higher abstract level of page category, which are representative of the structure of the website. The categories are: `frontpage`, `news`, `tech`, `local`, `opinion`, `on-air`, `misc`, `weather`, `health`, `living`, `business`, `sports`, `summary`, `BBS` (bulletin board

³archive.ics.uci.edu

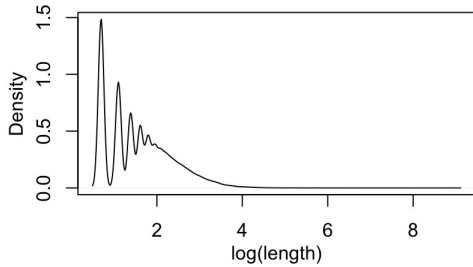


Figure 10: Sequences log-length distribution on msnbc.com

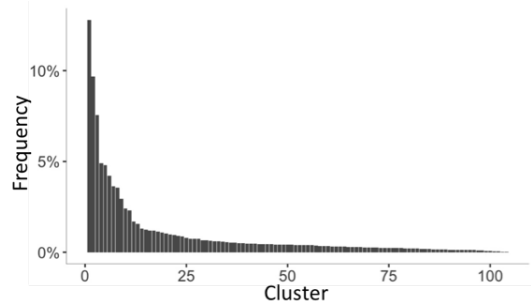


Figure 11: Frequency distribution of number of members in msnbc.com user clusters.

service), `travel`, `MSN-news`, and `MSN-sports`. The dataset comprises of 989,818 weblogs (sequences), of which we use a random sample of 100,000 sequences for our analysis. As expected, the distribution of sequence lengths (shown in Fig. 10, the distribution of log of sequence lengths) is found to be skewed and multi-modal. Their average length is 6.9 and standard deviation is 27.3, with range between 2 and 7440.

Our objective is to group the users with similar navigation patterns, irrespective of differences in their session lengths, into clusters. We, therefore, take the *length-insensitive* SGT version and use the random search procedure suggested in Sec. 3 to determine the optimal number of user clusters. In the procedure, we used k-means clustering with manhattan distance, and the goodness-of-fit criterion as db-index (Davies and Bouldin, 1979). The optimal point is found for the tuning parameter, $\kappa = 9$, and the number of clusters, $n_c = 104$.

The frequency distribution of number of members in each cluster is shown in Fig. 11. Again, as expected, the frequency distribution is like Pareto — majority of users belong to a small set of clusters. Nevertheless, it is important to understand distinct behaviors of both majority and minority users for better personalized services. Although most clusters have small memberships, but with huge amount of user sessions everyday, optimizing advertisements, marketing or design strategies, personalized to each group of users types (by their behavior) can bring significant improvement in returns.

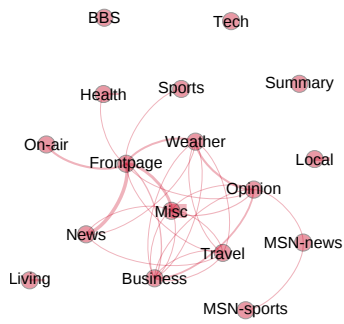
In Cadez et al. (2000), the optimal number of clusters for a sample of same size was found to be 100, close to our finding. However, the overall clustering results from Cadez et al. may have inconsistencies due to a first-order Markovian assumption. We ran hypothesis tests on the sequence data for verifying the assumption. The Markov tests result show majority of the data, about 67.9%, could not be tested, either due to the sequence’s short length or presence of single event throughout the sequence. Of the remaining, about 27% follows first order Markov property, and the rest has second or higher orders. Thus, applying Markov model based clustering on such data can be ineffective, on the other hand, proposed SGT based clustering does not depend on any distributional assumptions, hence, is better capable in identifying similar sequences.

5.2 Visualization

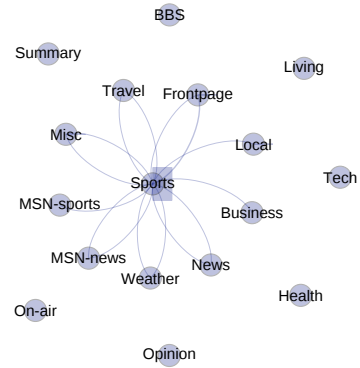
Effective visualization is a critical need for easy interpretation of a data and underlying properties. For example, in the above msnbc.com navigation data analysis, interpreting behavior of different user clusters is as important. The SGT’s graph equivalence provides an appropriate visualization technique.

In the following (Fig. 12a-12d), we show graph visualization of some clusters’ centroids, because a centroid represents the behavior of users present in the cluster. We have filtered edges with small weights for a better visualization. Thus, weakly connected nodes, i.e. infrequently visited pages, are seen as isolated.

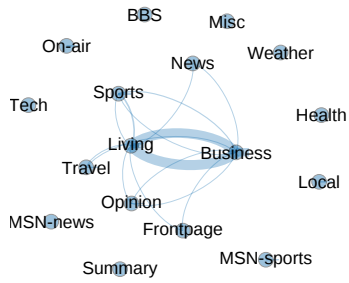
The representative SGT for the first cluster is shown in Fig. 12a. This cluster contains the highest membership (~12%), thus, indicates the “most” general behavior. The behavior graph in this group is centered around `frontage` and `misc`, with users tendency to navigate between `frontpage`, `misc`, `weather`, `opinion`, `news`, `travel` and `business`. Besides, users also tend to go to `on-air`, `health`, `sports` and `msn-news/sports` before leaving the website.



(a) Cluster# 1



(b) Cluster# 3



(c) Cluster# 25



(d) Cluster# 31

Figure 12: Graphical visualization of cluster representatives, showing user behaviors.

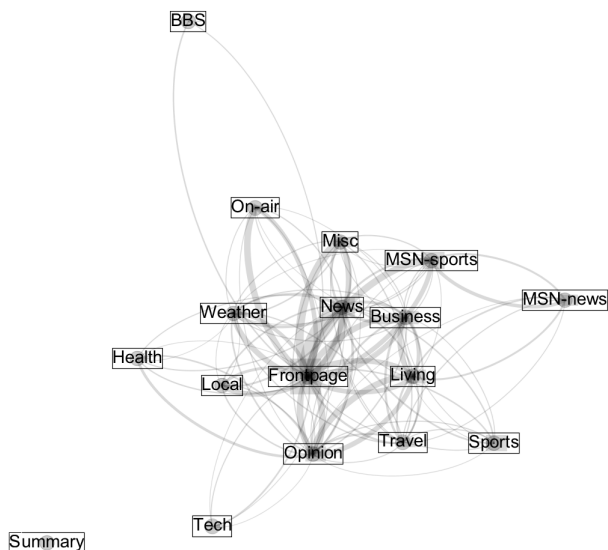


Figure 13: General navigation behavior of users on msnbc.com.

Fig. 12b shows another majority cluster with about 7.5% membership. This group of users seem to have a liking for sports. They primarily visit `sports` related pages (the box around `sports` node indicate a self-visiting edge), and also move back-and-forth from `sports` to `frontpage`, `travel`, `misc`, `msn-sports/news`, `weather`, `news`, `business`, and `local`.

Further, in Fig. 12c and 12d, we show two clusters with memberships of about 1%. The user behavior in both clusters are similar and different. In cluster-25, the users primary interest is centered around `living` and `business`, while in cluster-31, it is centered around `living` and `travel`. Thus, it can be interpreted that users having the former behavior are involved in more business and visit `living` pages for general daily and local living information, while the latter behavior indicates the users are interested in travel and living information of different places (not local).

While the clustering approach in the previous section (Sec. 5.1) provided us with cluster of users, the visualization shown in this section aids in understanding the user behaviors in each cluster. Besides, we did another analysis on the data, by considering the entire sample as one cluster (unit). This analysis will give us a general picture of user navigation behavior (see Fig. 13). It is observed that `summary` is the least visited category followed by `BBS` and `tech`. The `tech` category is mostly visited from `frontpage` and `news`, and counter-intuitively significantly often from `opinion` than `business`.

5.3 Classification

At many occasions we have labeled sequence data where it is required to build a classification model that can accurately assign a new sequence to the right class. Here we show that SGT representation can be used for building sequence classifiers. We use two datasets, a) protein sequences and its function as labels, and b) network intrusion data containing audit logs and attack labels.

The protein dataset is a sample of 2113 sequences taken from www.uniprot.org, where a sequence is from 20 alphabets (amino acids). Each sequence has one of two functions, viz. “Might take part in the signal recognition particle (SRP) pathway” and “Binds to DNA and alters its conformation”. These functions are treated as the sequence labels, and have almost a balanced distribution ($\sim 46.4\%$ for the first function). Besides, the sequence lengths in this dataset are similar, in the range of (289, 300). For this problem we use the *length-insensitive* SGT.

Another real world problem considered here is detection of intrusion in a computer network from the audit data. We use a sample of audit data with labels for an attack (positive class) or a normal event from MIT

SVM on- $\{\gamma_{protein}; \gamma_{network}\}$, $c = 1$	F1-score (#Features/SVs)	
	Protein data	Network intrusion
SGT $\{0.0014; 0.1\}$	99.61% (400/120)	89.65% (2,401/28)
Bag-of-words $\{0.05; 0.02\}$	88.45% (20/35)	48.32% (49/48)
2-gram $\{0.0025; 0.00041\}$	93.87% (400/45)	63.12% (2,401/25)
3-gram $\{0.00012; 8.4e - 06\}$	95.12% (8,000/202)	49.09% (117,649/29)
1+2-gram $\{0.0012; 0.0004\}$	94.34% (820/28)	64.39% (2,450/26)
1+2+3-gram $\{4.02e - 05; 8.32e - 06\}$	96.89% (24,820/15)	49.74% (120,099/27)

Table 2: Classification accuracy (F1-score) based on 10-fold cross validation results. # Features is dimension of input data to SVM, and SVs is the number of support vectors selected.

Lincoln Laboratory⁴. The dataset contains a BSM log file with about 400,000 lines, after post-processing gives event sequences for 115 sessions. There are 49 event types, corresponding to the alphabets set. The session lengths vary over a wide range of (12, 1773) with mean and standard deviation of (179, 192). Besides, since network intrusions are a rare event, the class distribution is significantly unbalanced with just 11.3% positive class data-points.

In this problem, we consider the sequence lengths as important (a *length-sensitive* problem), because sequences with similar pattern but different lengths can have different labels. Take a simple example of following two sessions: $\{\text{login, password, login, password, mail, ...}\}$ and $\{\text{login, password, ... (repeated several times) ..., login, password}\}$, while the first session can be a regular user mistyping the password once, the other session is possibly an attack to guess the password. Thus, the sequence lengths are as important as the patterns.

For both datasets, we first transformed the sequences to vectors using SGT, length-insensitive and -sensitive for protein ($\kappa = 1$) and network intrusion ($\kappa = 10$) data, respectively. For the network intrusion data, the sparsity of SGTs were high. Therefore, we performed principal component analysis (PCA) on it, and kept the top 10 PCs as sequence features, we call it SGT-PC, for further modeling.

After obtaining the SGT (-PC) features, we trained a SVM classifier on them. For comparison with commonly used sequence classifier techniques, we implemented bag-of-words (1-gram), 2-, 3-, 1+2-, 1+2+3-gram methods. The SVM was built with a RBF kernel. The cost parameter, c , is equal to 1, while the value for kernel parameter, γ , is shown within braces in Table 2. F1-score is used as a measure of accuracy, especially due to the network intrusion dataset where both precision and recall are important. The average test accuracy (F1-score) from a 10-fold cross validation is reported in the Table 2. Besides, the dimension of the data fed into SVM and the number of support vectors selected during training are shown as, “#Features” and “SVs”, respectively.

As we can see in Table 2, the F1-scores are high for all methods in protein data, with SGT based SVM surpassing all others, followed by 1+2+3-gram. On the other hand, the accuracies are small for the network intrusion data. This is primarily because of, a) a small dataset but high dimension (related to the alphabets size), leading to a weak predictive ability of models, and b) a few positive class examples (unbalanced data) causing a poor recall rate. Still, SGT outperformed other methods with a significant margin. Although the accuracies of the methods can be further increased using other classifiers, like Boosting, Random Forest, etc., it is beyond the scope of this paper. Here our purpose is to make a simplistic comparison to highlight the superiority of SGT features in building a supervised learning model.

5.4 Search

Most sequence databases found in real world are very large. For example, protein databases have billions of sequences and increasing. This increasing size has made it even more challenging to search for similar sequences (homologous) for structure or function predictions. Here we show that SGT sequence features can lead to a fast and accurate sequence search.

We collected a random sample of 1000 protein sequences from UniProtKB database on www.uniprot.org. To incorporate the protein sequence lengths for finding similarities, we transform them to Euclidean space using

⁴<https://www.ll.mit.edu/ideval/data/1998data.html>

length-sensitive SGT (with $\kappa = 1$). Thereafter, to reduce the dimension we applied principal component analysis, and preserved the first 40 principal components (explaining $\sim 83\%$ of variance), denoted by SGT-PC. We arbitrarily chose a protein sequence, Q9ZIM1⁵, as the search query. Note that here we denote a protein by its commonly used entry IDs (for eg. Q9ZIM1 used before) in the UniProtKB database.

We compute the Euclidean distance (specifically, the manhattan distance) between the SGT-PCs of the query and each sequence in the dataset. The top 10 closest sequences are shown with their SGT-PC distances in Table 3. As a reference, we also show the *identity* between the closely found sequences and the query. An identity between two protein sequences is the edit distance between them after alignment. Here we find identities after a global alignment, and cost of gap-opening as 0 and gap-extension as 1. Note that alignment algorithms are approximate heuristics, thus its results should be used only as a guideline, and not ground truth.

We find that the maximum pairwise identity (=46.3%) corresponds to the smallest SGT-PC distance (33.02) for {Q9ZIM1 (query), S9A4Q5}. Also, the identity level decreases with increasing SGT-PC differences, with some minor inconsistencies. Importantly, the computation time for finding SGT-PC differences between query and the entire dataset was 0.0014 sec on a 2.2GHz Intel Core i7 processor, while identity computations took 194.4 sec. Although, the currently in-use methods for protein databases, like BLAST, have a faster alignment and identity computation procedure than a pairwise, it will still be higher than finding vector differences.

If SGT-PC based search is implemented simply like above — find distance from each datapoint in the database —, the runtime increases linearly. We saw runtime increase of about 1000 times to 1.3 sec (from 0.0014 sec) on performing the distance computation on 1 million data-points. In practice, advanced techniques can be employed, for eg. similar to k-clust or HHblits, where the sequences are clustered and a cluster has a representative sequence or profile with which the query sequence is compared hierarchically. This reduces the search space — significantly reducing the runtime. Moreover, a parallel architecture can be added to divide the computation across several computing nodes. We leave these advancements for future research.

This concludes our case study, where we showed the application of SGT based sequence mining on real world problems and its compatibility with various distance and graph based data mining tools. In the next section we will discuss our results from this section and Sec. 4.

6 Discussion and Conclusion

As we showed in Sec. 2.4, SGT’s ability to capture the overall pattern — short and long range structures — of a sequence into a fixed finite-dimensional space makes it stand out. The n-gram models had lower performance than SGT because of this reason. N-grams cannot explicitly capture long-range dependencies, unless n is large, in which case the feature space becomes extremely large to handle.

Besides, the Markov models were outperformed due to their restrictive Markovian assumption, which was not always true for the data. Moreover, due to this assumption, these Markov models cannot effectively handle inherent stochasticities in a sequence and assess the long-range patterns. For illustration, suppose we have sequences in which “B occurs *closely* after A”. Consider one such example, **ABCDEAB**: a first-order Markov model will give a high transition probability (a feature), equal to one, that will correspond to the inherent pattern. But in presence of noise, for eg. a random alphabet, **X**, appearing in between A and B, **ABCDEAXB**, the transition probability will decrease by 50% (from 1.0 to 0.5). On the other hand, SGT is

Query, Q9ZIM1		
Protein	SGT-PC	Identity
S9A4Q5	33.02	46.3%
S8TYW5	34.78	46.3%
A0A029UVD9	39.21	45.1%
A0A030I738	39.34	45.1%
A0A029UWE3	39.41	45.1%
A0A029TT10	39.90	45.1%
G6N1A7	44.29	45.8%
J1GZY3	44.49	45.8%
F9M004	44.58	45.8%
M2CL02	44.61	44.3%

Table 3: Protein search query result from a sample dataset of size 1000.

⁵The protein sequence of Q9ZIM1 is, MSYQQQQCKQPCQPPVCPPTPKCEPCPPPKCEPYLPPPCPEHCPPPPCQDKCPCPVQPYPCQKQYPPKSK

robust to such noises. As shown in Fig.14, the percentage change in the SGT feature for (A,B), in the above case, is smaller than the Markov and decreases with increasing κ . It also shows that we can easily regulate the effect of such stochasticity, with a caution that sometimes the interspersed alphabets may not be noise but part of the sequence’s pattern (thus, we should not set κ as a high value without a validation).

Furthermore, a Markov model cannot easily distinguish between these two sequences: **ABCDEAB** and **ABCDEFGHIJAB**, from the (A,B) transition probabilities. In both sequences, the transition probability will be equal to 1, while the SGT feature for (A,B) changes from 1.72 to 2.94 ($\kappa = 1$), showing SGT’s capability in capturing the overall pattern. On another note, although deep learning methods can capture such overall patterns, their representations are in an arbitrary and usually very high dimension.

Thus, SGT proves to be more proficient in capturing sequence patterns. This, aided with the new possibility of using mainstream data mining techniques for sequence analysis, led to SGT outperforming other state-of-the-art sequence mining methods (see Sec. 4-5). Moreover, SGT also performs better in runtime. This is because, although SGT’s runtime upper-bound is proportional to the square of sequence length or alphabet set size, the actual runtime can be significantly lowered by few pre-processing. For example, on implementing Algorithm-2, we can first pre-process a sequence to obtain the list of positions of each alphabet, and then run a nested loop *only* for the alphabets present in the sequence.

In addition, SGT’s unique property of including or excluding the sequence length effect makes it compatible for both length sensitive and insensitive sequence problems. We show its efficacy by performing real world data analysis for both cases.

In summary, SGT is a novel approach to perform effective feature extraction on any sequence to give it a finite-dimensional representation in a Euclidean space. This bridges an existing gap between sequence problems and powerful mainstream data mining methods. Moreover, it has been shown to have a universal applicability to many sequence problems with various applications. Importantly, due to its low computational complexity and ease of parallelization it can be scaled to most big sequence data problem. For future research, we should attempt to use SGT to develop new methods for diverse sequence problems in speech recognition, text analysis, bioinformatics etc., or use it as an embedding layer in deep learning architectures.

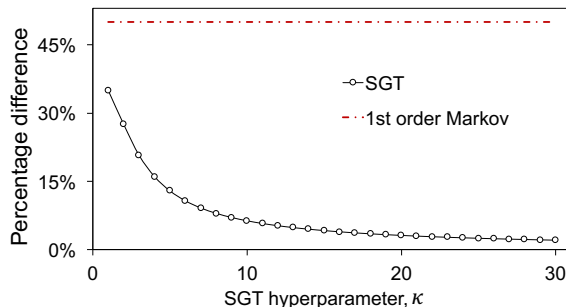


Figure 14: Percentage change in SGT feature for (A,B) with κ in presence of a noise.

References

- [1] Altschul, S. F., Madden, T. L., Schäffer, A. A., Zhang, J., Zhang, Z., Miller, W., and Lipman, D. J. (1997). Gapped blast and psi-blast: a new generation of protein database search programs. *Nucleic acids research*, 25(17):3389–3402.
- [2] Cadez, I., Heckerman, D., Meek, C., Smyth, P., and White, S. (2003). Model-based clustering and visualization of navigation patterns on a web site. *Data Mining and Knowledge Discovery*, 7(4):399–424.
- [3] Comin, M. and Verzotto, D. (2012). Alignment-free phylogeny of whole genomes using underlying subwords. *Algorithms for Molecular Biology*, 7(1):1.
- [4] Davies, D. L. and Bouldin, D. W. (1979). A cluster separation measure. *IEEE transactions on pattern analysis and machine intelligence*, (2):224–227.
- [5] Didier, G., Corel, E., Laprevotte, I., Grossmann, A., and Landés-Devauchelle, C. (2012). Variable length local decoding and alignment-free sequence comparison. *Theoretical Computer Science*, 462:1–11.
- [6] Ding, C. H. and Dubchak, I. (2001). Multi-class protein fold recognition using support vector machines and neural networks. *Bioinformatics*, 17(4):349–358.

- [7] Dong, G. and Pei, J. (2007). *Sequence data mining*, volume 33. Springer Science & Business Media.
- [8] Edgar, R. C. (2004). Muscle: a multiple sequence alignment method with reduced time and space complexity. *BMC bioinformatics*, 5(1):1.
- [9] Edgar, R. C. (2010). Search and clustering orders of magnitude faster than blast. *Bioinformatics*, 26(19):2460–2461.
- [10] Fu, L., Niu, B., Zhu, Z., Wu, S., and Li, W. (2012). Cd-hit: accelerated for clustering the next-generation sequencing data. *Bioinformatics*, 28(23):3150–3152.
- [11] Gaber, M. M. (2009). *Scientific data mining and knowledge discovery*. Springer.
- [12] Graves, A. (2013). Generating sequences with recurrent neural networks. *arXiv preprint arXiv:1308.0850*.
- [13] Han, J., Pei, J., Mortazavi-Asl, B., Pinto, H., Chen, Q., Dayal, U., and Hsu, M. (2001). Prefixspan: Mining sequential patterns efficiently by prefix-projected pattern growth. In *proceedings of the 17th international conference on data engineering*, pages 215–224.
- [14] Hauser, M., Mayer, C. E., and Söding, J. (2013). kclust: fast and sensitive clustering of large protein sequence databases. *BMC bioinformatics*, 14(1):1.
- [15] Helske, S. and Helske, J. (2016). Mixture hidden markov models for sequence data: the seqhmm package in r.
- [16] Kumar, P., Krishna, P. R., and Raju, S. B. (2012). *Pattern discovery using sequence data mining: applications and studies*. Information Science Reference.
- [17] Linial, M., Linial, N., Tishby, N., and Yona, G. (1997). Global self-organization of all known protein sequences reveals inherent biological signatures. *Journal of molecular biology*, 268(2):539–556.
- [18] Needleman, S. B. and Wunsch, C. D. (1970). A general method applicable to the search for similarities in the amino acid sequence of two proteins. *Journal of molecular biology*, 48(3):443–453.
- [19] Pearson, W. R. (1990). Rapid and sensitive sequence comparison with fastp and fasta. *Methods in enzymology*, 183:63–98.
- [20] Ranjan, C., Paynabar, K., and Helm, J. E. (2015). A new semi-markov model based clustering for a clustering-scheduling integrated framework for patient flow modeling and optimization. *arXiv preprint arXiv:1505.07752*.
- [21] Remmert, M., Biegert, A., Hauser, A., and Söding, J. (2012). Hhblits: lightning-fast iterative protein sequence searching by hmm-hmm alignment. *Nature methods*, 9(2):173–175.
- [22] Siyari, P., Dilkina, B., and Dovrolis, C. (2016). Lexis: An optimization framework for discovering the hierarchical structure of sequential data. *arXiv preprint arXiv:1602.05561*.
- [23] Smith, T. F. and Waterman, M. S. (1981). Identification of common molecular subsequences. *Journal of molecular biology*, 147(1):195–197.
- [24] Tomović, A., Janičić, P., and Kešelj, V. (2006). n-gram-based classification and unsupervised hierarchical clustering of genome sequences. *Computer methods and programs in biomedicine*, 81(2):137–153.

Appendices

Appendix A: Arithmetico-Geometric series

The sum of a series, where the k^{th} term for $k \geq 1$ can be expressed as,

$$t_k = (a + (k - 1)d) br^{k-1}$$

is called as an arithmetico-geometric because of a combination of arithmetic series term $(a + (k - 1)d)$, where a is the initial term and common difference d , and geometric br^{k-1} , where b is the initial value and common ratio being r .

Suppose the sum of the series till n terms is denoted as,

$$S_n = \sum_{k=1}^n (a + (k - 1)d) br^{k-1} \quad (13)$$

Without loss of generality we can assume $b = 1$ for deriving the expression for S_n (the sum for any other value of b can be easily obtained by multiplying the expression for S_n with b). Expanding Eq. 13,

$$S_n = a + (a + d)r + (a + 2d)r^2 + \dots + (a + (n - 1)d)r^{n-1} \quad (14)$$

Now multiplying S_n with r ,

$$rS_n = ar + (a + d)r^2 + (a + 2d)r^3 + \dots + (a + (n - 1)d)r^n \quad (15)$$

Subtracting Eq. 15 from 14, if $|r| < 1$, else we subtract the latter from the former, we get,

$$\begin{aligned} |(1 - r)S_n| &= \left| [a + (a + d)r + (a + 2d)r^2 + \dots + (a + (n - 1)d)r^{n-1}] \right. \\ &\quad \left. - [ar + (a + d)r^2 + (a + 2d)r^3 + \dots + (a + (n - 1)d)r^n] \right| \\ &= \left| a + d(r + r^2 + \dots + r^{n-1}) - (a + (n - 1)d)r^n \right| \\ &= \left| a + \frac{dr(1 - r^{n-1})}{1 - r} - (a + (n - 1)d)r^n \right|. \end{aligned}$$

Therefore,

$$S_n = \left| \frac{1}{1 - r} \left[a + \frac{dr(1 - r^{n-1})}{1 - r} - (a + (n - 1)d)r^n \right] \right| \quad (16)$$

or, for any value of b ,

$$S_n = b \left| \frac{1}{1 - r} \left[a + \frac{dr(1 - r^{n-1})}{1 - r} - (a + (n - 1)d)r^n \right] \right| \quad (17)$$

Appendix B: Mean and Variance of a graph transform feature, ψ_{uv} .

To easily denote various (u, v) pairs in Fig. 4, we use a term, m -th neighboring pair, where an m -th neighbor pair for (u, v) will have $m - 1$ other u 's in between. A first neighbor, is thus, the immediate (u, v) neighboring pairs, while the 2nd-neighbor has one other u in between, and so on. See Fig. 15 for an illustration on the example in Fig. 4. The *immediate* neighbors mentioned in the assumption in Sec. 2.4 is same as the first neighbor defined here.

The following derivation follows the assumptions made in Sec. 2.4. In addition to the variables mentioned in the assumptions, we represent the expected number of first-neighbor (u, v) pairs as,

$$M = pL \quad (18)$$

Consequently, it is easy to show that the expected number of m -th neighboring (u, v) pairs is $(M - m + 1)$, i.e., second neighboring (u, v) pairs will be $(M - 1)$, $(M - 2)$ for the third, so on and so forth, till one instance for the M^{th} neighbor (see Fig. 15 for an example). The gap distance for an m^{th} neighbor is given as,

$$Z_1 = X \quad ; \quad Z_m = X + \sum_{i=2}^m Y_i, m = 2, \dots, M \quad (19)$$

Besides, the total number of (u, v) pair instances will be $\sum_{m=1}^M m = \frac{M(M+1)}{2}$ ($= |\Lambda_{uv}|$, by definition). Suppose, we define a set that contains distances for each possible (u, v) pairs, as $\mathcal{Z} = \{Z_m^i, i = 1, \dots, (M - m + 1); m = 1, \dots, M\}$.

Thus, putting these into Eq. 3a, the feature, ψ_{uv} can also be expressed as, $\psi_{uv} = \frac{\sum_{Z \in \mathcal{Z}} \phi_\kappa(Z)}{|\Lambda_{uv}|}$.

Also, since $Z \sim N(\mu_d, \sigma_d^2)$, the developer function $\phi_\kappa(Z)$ becomes a lognormal distribution.

$$\phi_\kappa(Z) \sim \text{lognormal}(\kappa\mu_d, \kappa^2\sigma_d^2) \quad (20)$$

Mean

Length-sensitive SGT

We first derive the expected value of ψ_{uv} for a length-sensitive SGT as,

$$\begin{aligned} E[\psi_{uv}] &= \frac{\sum_{Z \in \mathcal{D}} E[\phi_\kappa(Z)]}{M(M+1)/2} \\ &= \frac{ME[\phi_\kappa(Z_1)] + (M-1)E[\phi_\kappa(Z_2)] + \dots + E[\phi_\kappa(Z_M)]}{M(M+1)/2} \\ &= \frac{\sum_{m=1}^M (M - (m-1))E[\phi_\kappa(Z_m)]}{M(M+1)/2} \end{aligned} \quad (21)$$

Since, X and Y are normally distributed, the pair gap-distance variable, Z in Eq. 19 will be,

$$Z_m \sim N(\mu_\alpha + (m-1)\mu_\beta, \sigma_\alpha^2 + (m-1)\sigma_\beta^2) \quad (22)$$

Therefore, $\phi_\kappa(Z_m) \sim \text{lognormal}$ (see Eq. 20), and

$$\begin{aligned} E[\phi_\kappa(Z_m)] &= e^{-\kappa(\mu_\alpha + (m-1)\mu_\beta) + \frac{1}{2}\kappa^2(\sigma_\alpha^2 + (m-1)\sigma_\beta^2)} \\ &= e^{-\tilde{\mu}_\alpha - (m-1)\tilde{\mu}_\beta} \end{aligned} \quad (23)$$

$$\begin{aligned} \text{var}[\phi_\kappa(Z_m)] &= \left(e^{\kappa^2(\sigma_\alpha^2 + (m-1)\sigma_\beta^2)} - 1 \right) e^{-2\kappa(\mu_\alpha + (m-1)\mu_\beta) + \kappa^2(\sigma_\alpha^2 + (m-1)\sigma_\beta^2)} \\ &= e^{-2\tilde{\mu}'_\alpha - 2(m-1)\tilde{\mu}'_\beta} - e^{-2\tilde{\mu}_\alpha - 2(m-1)\tilde{\mu}_\beta} \end{aligned} \quad (24)$$

where,

$$\begin{aligned} \tilde{\mu}_\alpha &= \kappa\mu_\alpha - \frac{\kappa^2}{2}\sigma_\alpha^2 \quad ; \quad \tilde{\mu}'_\alpha = \kappa\mu_\alpha - \kappa^2\sigma_\alpha^2 \\ \tilde{\mu}_\beta &= \kappa\mu_\beta - \frac{\kappa^2}{2}\sigma_\beta^2 \quad ; \quad \tilde{\mu}'_\beta = \kappa\mu_\beta - \kappa^2\sigma_\beta^2 \end{aligned} \quad (25)$$

Substituting the results in Eq. 23 to Eq. 21 and Eq. 16 from Appendix A, we get,

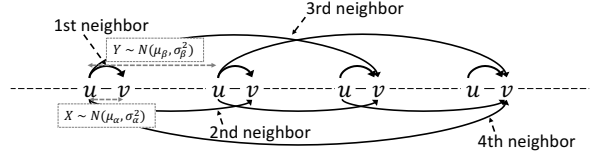


Figure 15: Illustration of notations used for SGT properties derivation

$$\begin{aligned}
E[\psi_{uv}] &= \frac{\sum_{m=1}^M (M - (m - 1)) e^{-\tilde{\mu}_\alpha - (m-1)\tilde{\mu}_\beta}}{M(M + 1)/2} \\
&= \left(\frac{2}{M + 1} \right) \left| \left(\frac{e^{-\tilde{\mu}_\alpha}}{1 - e^{-\tilde{\mu}_\beta}} \right) \left[1 - \frac{1}{M(e^{\tilde{\mu}_\beta} - 1)} (1 - e^{-M\tilde{\mu}_\beta}) \right] \right| \\
&= \frac{2}{pL + 1} \left| \frac{e^{-\tilde{\mu}_\alpha}}{(1 - e^{-\tilde{\mu}_\beta}) \left[1 - \frac{1 - e^{-pL\tilde{\mu}_\beta}}{pL(e^{\tilde{\mu}_\beta} - 1)} \right]} \right| \\
&= \frac{2}{pL + 1} \gamma
\end{aligned} \tag{26}$$

where,

$$\gamma = \left| \frac{e^{-\tilde{\mu}_\alpha}}{(1 - e^{-\tilde{\mu}_\beta}) \left[1 - \frac{1 - e^{-pL\tilde{\mu}_\beta}}{pL(e^{\tilde{\mu}_\beta} - 1)} \right]} \right| \tag{27}$$

Length-insensitive SGT

Next, as given in Eq. 3b for the length insensitive sequence problem, Λ_{uv} is normalized by the sequence length. Thus, the edge weight, $E[\psi_{uv}]$ will be,

$$\begin{aligned}
E[\psi_{uv}] &= \frac{\sum_{m=1}^M (M - (m - 1)) e^{-\tilde{\mu}_\alpha - (m-1)\tilde{\mu}_\beta}}{\left(\frac{M(M+1)/2}{L} \right)} \\
&= \frac{2L}{pL + 1} \gamma
\end{aligned} \tag{28}$$

Variance

Length-sensitive SGT

The variance of an edge feature, ψ_{uv} , can be computed as,

$$\begin{aligned}
\text{var}(\psi_{uv}) &= \left(\frac{1}{M(M + 1)/2} \right)^2 \sum_{m=1}^M (M - (m - 1)) \left[e^{-2\tilde{\mu}'_\alpha - 2(m-1)\tilde{\mu}'_\beta} - e^{-2\tilde{\mu}_\alpha - 2(m-1)\tilde{\mu}_\beta} \right] \\
&= \left(\frac{1}{M(M + 1)/2} \right)^2 \left[\underbrace{\sum_{m=1}^M (M - (m - 1)) e^{-2\tilde{\mu}'_\alpha - 2(m-1)\tilde{\mu}'_\beta}}_{V_1} - \underbrace{\sum_{m=1}^M (M - (m - 1)) e^{-2\tilde{\mu}_\alpha - 2(m-1)\tilde{\mu}_\beta}}_{V_2} \right]
\end{aligned} \tag{29}$$

Again, both V_1 and V_2 forms an Arithmetico-Geometric series. Solving for them, we get,

$$\begin{aligned}
V_1 &= \sum_{m=1}^M (M - (m - 1)) e^{-2\tilde{\mu}'_\alpha - 2(m-1)\tilde{\mu}'_\beta} \\
&= e^{-2\tilde{\mu}'_\alpha} \sum_{m=1}^M (M - (m - 1)) e^{-2(m-1)\tilde{\mu}'_\beta} \\
&= \frac{e^{-2\tilde{\mu}'_\alpha}}{1 - e^{-2\tilde{\mu}'_\beta}} \left[M - e^{-2\tilde{\mu}'_\beta} \left(\frac{1 - e^{-2(M-1)\tilde{\mu}'_\beta}}{1 - e^{-2\tilde{\mu}'_\beta}} \right) - (M - (M - 1)) e^{-2M\tilde{\mu}'_\beta} \right] \\
&= \frac{e^{-2\tilde{\mu}'_\alpha}}{1 - e^{-2\tilde{\mu}'_\beta}} \left[M - e^{-2\tilde{\mu}'_\beta} \left(\frac{1 - e^{-2M\tilde{\mu}'_\beta}}{1 - e^{-2\tilde{\mu}'_\beta}} \right) \right]
\end{aligned} \tag{30}$$

Similarly,

$$\begin{aligned}
V_2 &= \sum_{m=1}^M (M - (m - 1)) e^{-2\tilde{\mu}_\alpha - 2(m-1)\tilde{\mu}_\beta} \\
&= \frac{e^{-2\tilde{\mu}_\alpha}}{1 - e^{-2\tilde{\mu}_\beta}} \left[M - e^{-2\tilde{\mu}_\beta} \left(\frac{1 - e^{-2M\tilde{\mu}_\beta}}{1 - e^{-2\tilde{\mu}_\beta}} \right) \right]
\end{aligned} \tag{31}$$

Therefore, plugging in Eq. 30-31 and Eq. 18 into Eq. 29, we get,

$$\begin{aligned}
\text{var}(\psi_{uv}) &= \left(\frac{1}{pL(pL + 1)/2} \right)^2 \left[\left\{ \frac{e^{-2\tilde{\mu}'_\alpha}}{1 - e^{-2\tilde{\mu}'_\beta}} \left(pL - e^{-2\tilde{\mu}'_\beta} \left(\frac{1 - e^{-2pL\tilde{\mu}'_\beta}}{1 - e^{-2\tilde{\mu}'_\beta}} \right) \right) \right\} \right. \\
&\quad \left. - \left\{ \frac{e^{-2\tilde{\mu}_\alpha}}{1 - e^{-2\tilde{\mu}_\beta}} \left(pL - e^{-2\tilde{\mu}_\beta} \left(\frac{1 - e^{-2pL\tilde{\mu}_\beta}}{1 - e^{-2\tilde{\mu}_\beta}} \right) \right) \right\} \right]
\end{aligned}$$

It is easy to show that,

$$\lim_{L \rightarrow \infty} \text{var}(\psi_{uv}) \rightarrow 0$$

Length-insensitive SGT

Besides, for length-insensitive case, the variance will be,

$$\begin{aligned}
\text{var}(\psi_{uv}) &= \left(\frac{1}{p(pL + 1)} \right)^2 \left[\left\{ \frac{e^{-2\tilde{\mu}'_\alpha}}{1 - e^{-2\tilde{\mu}'_\beta}} \left(pL - e^{-2\tilde{\mu}'_\beta} \left(\frac{1 - e^{-2pL\tilde{\mu}'_\beta}}{1 - e^{-2\tilde{\mu}'_\beta}} \right) \right) \right\} \right. \\
&\quad \left. - \left\{ \frac{e^{-2\tilde{\mu}_\alpha}}{1 - e^{-2\tilde{\mu}_\beta}} \left(pL - e^{-2\tilde{\mu}_\beta} \left(\frac{1 - e^{-2pL\tilde{\mu}_\beta}}{1 - e^{-2\tilde{\mu}_\beta}} \right) \right) \right\} \right]
\end{aligned}$$

which also has limiting value of 0 as the sequence length increases, at the rate of $1/L$.

$$\lim_{L \rightarrow \infty} \text{var}(\psi_{uv}) \xrightarrow{1/L} 0$$

Appendix C: Proof for SGT expression for undirected sequences

Proof for Eq. 11:

By definition,

$$\Lambda_{uv}(s) = \{(l, m) : x_l = u, x_m = v, l < m, (l, m) \in 1, \dots, L^{(s)}\}$$

Similarly, Λ_{uv} can be expressed as,

$$\begin{aligned} \Lambda_{uv}(s) &= \{(l, m) : x_l = u, x_m = v, l > m, (l, m) \in 1, \dots, L^{(s)}\} \\ &= \Lambda_{vu}^T(s) \end{aligned}$$

Next, Eq. 9 can be expanded as,

$$\begin{aligned} \tilde{\Lambda}_{uv}(s) &= \{(l, m) : x_l = u, x_m = v, (l, m) \in 1, \dots, L^{(s)}\} \\ &= \{(l, m) : x_l = u, x_m = v, l < m, (l, m) \in 1, \dots, L^{(s)}\} \\ &\quad + \{(l, m) : x_l = u, x_m = v, l > m, (l, m) \in 1, \dots, L^{(s)}\} \\ &= \Lambda_{uv}(s) + \Lambda_{uv}^T(s) \end{aligned}$$

Thus, proving Eq. 10. Next, the SGT for undirected sequence in Eq. 11, can be expressed as,

$$\begin{aligned} \tilde{\Psi}_{uv}(s) &= \frac{\sum_{\forall(l,m) \in \tilde{\Lambda}_{uv}(s)} \phi_\kappa(d(l, m))}{|\tilde{\Lambda}_{uv}(s)|} \\ &= \frac{\sum_{\forall(l,m) \in \Lambda_{uv}(s)} \phi_\kappa(d(l, m)) + \sum_{\forall(l,m) \in \Lambda_{uv}^T(s)} \phi_\kappa(d(l, m))}{|\Lambda_{uv}(s)| + |\Lambda_{uv}^T(s)|} \\ &= \frac{|\Lambda_{uv}(s)|\Psi_{uv}(s) + |\Lambda_{uv}^T(s)|\Psi_{uv}^T(s)}{|\Lambda_{uv}(s)| + |\Lambda_{uv}^T(s)|} \end{aligned}$$

Thus, proving Eq. 11.

Appendix D: Proof for Alphabet Clustering

We have,

$$\begin{aligned} \frac{\partial \Delta}{\partial \kappa} &= \frac{\partial}{\partial \kappa} E[\phi_\kappa(X) - \phi_\kappa(Y)] \\ &= E\left[\frac{\partial}{\partial \kappa} \phi_\kappa(X) - \frac{\partial}{\partial \kappa} \phi_\kappa(Y)\right] \end{aligned} \tag{32}$$

For $E[X] < E[Y]$, we want, $\frac{\partial \Delta}{\partial \kappa} > 0$, in turn, $\frac{\partial}{\partial \kappa} \phi_\kappa(X) > \frac{\partial}{\partial \kappa} \phi_\kappa(Y)$ (from Eq. 32). This will hold, if

$$\frac{\partial^2}{\partial d \partial \kappa} \phi_\kappa(d) > 0 \tag{33}$$

that is, slope, $\frac{\partial}{\partial \kappa} \phi_\kappa(d)$ is increasing with d . For an exponential expression for ϕ (Eq. 1, the condition in Eq. 33 holds true if $\kappa d > 1$. Hence, under these conditions, the *separation* increases as we increase the tuning parameter, κ .